NeuroToxicology 54 (2016) 111–118

Contents lists available at ScienceDirect

NeuroToxicology

Full length article

# Caveolae as a target for *Phoneutria nigriventer* spider venom

Edilene Siqueira Soares[a], Monique Culturato Padilha Mendonça[a,b], Maria Alice da Cruz-Höfling[a,b,*]

[a] Department of Biochemistry and Tissue Biology, Institute of Biology, State University of Campinas (UNICAMP), 13083-970 Campinas, SP, Brazil
[b] Department of Pharmacology, Faculty of Medical Sciences, State University of Campinas (UNICAMP), 13083-970 Campinas, SP, Brazil

ARTICLE INFO

*Article history:*
Received 30 July 2015
Received in revised form 1 April 2016
Accepted 5 April 2016
Available online 6 April 2016

*Keywords:*
Blood-brain barrier breakdown
Caveolae
Spider venom
Vesicle trafficking

ABSTRACT

An important transcellular transport mechanism in the blood-brain barrier (BBB) involves caveolae, which are specialized delta-shaped domains of the endothelial plasma membrane that are rich in cholesterol, glycosphingolipids and the scaffolding protein Caveolina-1 (Cav-1). In this work, we investigated whether the increase in endocytosis and transendothelial vesicular trafficking in rat cerebellum after blood-brain barrier breakdown (BBBb) induced by *Phoneutria nigriventer* spider venom (PNV) was mediated by caveolae. The expression of Cav-1, phosphorylated Cav-1 (pCav-1), dynamin-2 (Dyn2), Src kinase family (SKF) and matrix-metalloproteinase-9 (MMP9), proteins involved in caveolar dynamics and BBB opening, was investigated. Immunofluorescence, western blotting (WB) and transmission electron microscopy were used to assess changes at 1, 2, 5, 24 and 72 h post-venom. WB showed upregulation of Cav-1, Dyn2 and MMP9 at 1, 5 and 72 h (corresponding, respectively, to intervals when intoxication was most evident, when signs of recovery were present, and when no intoxication was detectable). In contrast, pCav-1 and SKF, which are essential for internalization and transport, decreased when Cav-1 and Dyn2, proteins essential for caveolar formation, were increased. Overall, these changes indicated that vesicular trafficking across the endothelium (high pCav/SKF levels) coincided with lower numbers of caveolae (Cav-1/Dyn2 downregulation) and lower expression of MMP9. Thus, the internalization (disassembly) of caveolae alternates with caveolar neoformation (assembly), resulting in changes in caveolar density in the endothelium membrane. These caveolar dynamics imply tensional mechanical stress that is important in triggering key signaling mechanisms. We conclude that PNV-induced breakdown of transcellular transport in the BBB is caused by an increase in caveolae-mediated endocytosis; this effect was correlated with the progression of temporal signs of envenoming. Caveolar dynamics are probably involved in shear stress and BBBb regulatory mechanisms in this experimental model.

© 2016 The Authors. Published by Elsevier Inc. This is an open access article under the CC BY-NC-ND license (http://creativecommons.org/licenses/by-nc-nd/4.0/).

## 1. Introduction

The venom of *Phoneutria nigriventer* (banana or wandering spider), a medically important spider in Brazil, contains a variety of pharmacologically-active neuropeptides, some of which activate or delay the inactivation of tetrodotoxin (TTX)-sensitive $Na^+$ channels; this modulation results in the depolarization of excitable membranes by increasing $Na^+$ influx and increase the stores of intracellular $Ca^{2+}$. *P. nigriventer* venom (PNV) also blocks $K^+$ channels and different types of $Ca^{2+}$ channels (Fontana and Vital-Brazil, 1985; Love et al., 1986; Gomez et al., 2002). The ability of PNV to interfere with ion channel physiology adversely affects neurotransmission, as shown by the modulation of glutamate release and glutamate uptake (see Gomez et al., 2002). The clinical manifestations of severe envenomation by *P. nigriventer* include pain, edema, intense sweating, muscle weakness, arterial hypertension, cardiac arrhythmias, respiratory distress, agitation, blurred vision and sometimes convulsions (Bucaretchi et al., 2000, 2008).

Various studies have shown that PNV disrupts the blood-brain barrier (BBB) and alters the expression of proteins related directlyor indirectly to barrier function (Le Sueur et al., 2003, 2004, 2005; da Cruz-Höfling et al., 2009; Mendonça et al., 2012, 2013, 2014; Rapôso et al., 2007, 2012, 2014; Stávale et al., 2013). PNV-induced BBB opening involves a marked increase in transcellular vesicle transport (Le Sueur et al., 2004, 2005)

*Abbreviations:* BBB, blood-brain barrier; BBBb, blood brain-barrier breakdown; Cav-1, caveolin-1; CNS, central nervous system; Dyn2, Dynamin-2; IF, immunofluorescence; MMP9, metalloproteinase-9; pCav-1, phosphorylated caveolin-1; PNV, *Phoneutria nigriventer* venom; SKF, Src tyrosine kinase family; TEM, transmission electron microcopy; WB, western blotting.

* Corresponding author.
*E-mail address:* hofling@unicamp.br (M.A. da Cruz-Höfling).

http://dx.doi.org/10.1016/j.neuro.2016.04.005
0161-813X/© 2016 The Authors. Published by Elsevier Inc. This is an open access article under the CC BY-NC-ND license (http://creativecommons.org/licenses/by-nc-nd/4.0/).

and redistribution of endothelial junction proteins (Rapôso et al., 2012; Mendonça et al., 2013). Augmented endothelial transcytosis in the brain microvessels of rats injected with PNV was seen as rows of flask-shaped indentations at the adluminal and abluminal surfaces of endothelial and smooth muscle cells of venules and arterioles. The finding that the indentations were loaded with lanthanum nitrate, a peripherally-injected extracellular tracer, indicated tracer uptake from the vessel lumen and vesicle trafficking across the endothelium with delivery of the vesicle to the interstitial spaces of the neuropil; cytotoxicity and vascular edema were also observed (Le Sueur et al., 2003, 2004). These flask-shaped indentations, known as caveolae, are cholesterol- and glycosphingolipid-rich membrane microdomains that compartmentalize many molecules, including caveolin, endothelial nitric oxide synthase, G proteins and phosphatases (Pattel et al., 2008).

Under physiological conditions, the BBB helps to maintain a stable microenvironment in the central nervous system (CNS) that ensures the proper functioning of neuronal and glia cells in brain homeostasis. Homeostasis of the CNS disrupts by many factors, including, but not limited to, endogenous neurodegenerative diseases and exogenous neurointoxication such as caused after envenomation by venomous animals.

Typically, the endothelium of the brain microcirculation possesses few caveolae, as high electrical resistance and highly receptor- and carrier-regulated transcytosis restrict transport at the BBB. Therefore, an increase in the number of caveolae after exposure to PNV implies venom-induced permeabilization of the BBB through impairment of the transcellular pathway. We have recently shown that PNV upregulates the expression of caveolin-1α (Cav-1), the main caveolar scaffolding protein, and increases the number of vessels labeled with Cav-1 and the number of Cav-1 positive Purkinje neurons in rat cerebellum (Soares et al., 2014). These findings suggest a role for Cav-1 in the increased endocytosis and transcytosis reported in earlier studies of PNV-induced BBB breakdown (Le Sueur et al., 2003, 2004) and a possible role in neuronal signaling (Stern and Mermelstein, 2010).

Caveolin coated-caveolae contribute to the regulation of cell membrane dynamics (Nassoy and Lamaze, 2012) and caveolae mediate the endocytosis and trafficking of substances by sorting transporting vesicles into the cell cytoplasm (Pelkmans and Helenius, 2002; Shajahan et al., 2004b). Increased transcytosis of plasma protein by endothelial caveolae has also been linked to BBB breakdown and cerebral edema (Nag et al., 2009). Caveolae-derived vesicle trafficking requires phosphorylation of Cav-1 (pCav-1) by activation of the Src kinase family (SKF) (Shajahan et al., 2004b; Nag et al., 2009) and dynamin-2 (Dyn2), a caveolae neck-forming protein with a role in caveolar scission and internalization (Yao et al., 2005); the activation of these proteins results in plasma membrane flattening (Henley et al., 1998).

The purpose of the present study was to investigate two proteins that have pivotal importance in caveolar structure and function, namely caveolin-1 and dynamin-2; we also assessed possible mechanistic pathways triggered in response to circulating PNV in rats. This work was done at specific intervals of envenoming, namely, (a) when intense manifestations of acute toxicity were present (1–2 h post-PNV), (b) when recovery was in progress (5 h post-PNV) and (c) when there were no clinical manifestations and the rats showed normal behavior (24–72 h post-PNV).

## 2. Materials and methods

### 2.1. P. nigriventer *venom (PNV)*

Lyophilized venom from *P. nigriventer* (PNV) was kindly donated by Dr. Evanguedes Kalapothakis (UFMG, Belo Horizonte, MG, Brazil) and stored at −20 °C. The venom was dissolved in 0.9% sterile saline solution (0.5 mg PNV/ml sterile saline) immediately prior to use.

### 2.2. Animals and envenoming procedure

Male Wistar rats (*Rattus norvegicus*) 6–7 weeks old were obtained from the Multidisciplinary Center for Animal Investigation (CEMIB) at UNICAMP (Campinas, SP, Brazil). They were maintained at a 12 h light-dark cycle (25–28 °C) with free access to food and drinking water until the experimental procedure was performed. A single intravenous (i.v.) injection of a sub-lethal dose of PNV (0.5 mg/kg) (Soares et al., 2015) was administered to rats (n = 55 total) that were subsequently killed at 1, 2, 5, 24 and 72 h post-PNV (n = 11/interval, i.e., n = 5 for western blotting and n = 3 for immunofluorescence and transmission electron microscopy per time interval). A single control group received the same volume of vehicle and was killed 5 h later (n = 11, i.e., n = 5 for western blotting and n = 3 for immunofluorescence and transmission electron microscopy). The experiments were approved by an institutional Committee for Ethics in Animal Use (CEUA/UNICAMP, protocol no. 3609-1) and were done in accordance with the general ethical guidelines of the Brazilian Society for Laboratory Animal Science (SBCAL).

### 2.3. Western blotting (WB)

After venom or saline treatment, the rats were killed in a $CO_2$ chamber and their brains removed and immediately frozen in liquid nitrogen. Brain proteins were subsequently separated in an extraction cocktail and run on 12% polyacrylamide gels in SDS-PAGE followed by electrotransfer to nitrocellulose membranes, as described elsewhere (Rapôso et al., 2012). The membranes were blocked overnight with 5% non-fat milk and incubated for 4 h with primary antibodies against caveolin-1 (1:1000), dynamin-2 (1:500), and metalloproteinase-9 (1:500), all from Santa Cruz Biotechnology (Santa Cruz, CA, USA), Src tyrosine kinase family (SKF, 1:1000) and *p*-caveolin-1 (1:1000), both from Cell Signaling Technology (Danvers, MA, USA) and β-actin (1:1000; Sigma-Aldrich, St. Louis, MO, USA). The membranes were then incubated with secondary antibodies: anti-rabbit (1:1000) for caveolin-1, SKF and *p*-caveolin-1, anti-goat (1:1000) for dynamin-2 and metalloproteinase-9, and anti-mouse for β-actin (1:40,000; all from Sigma-Aldrich). Proteins bands were visualized by chemiluminescence (Thermo Scientific, Waltham, MA, USA) and band intensity was quantified by measuring the density of pixels of each band using Image J 1.45 s program (Wayne Rasband, NIH, Bethesda, MD, USA). The experiments were performed in a set of three replicates. The quantifications were normalized against the corresponding value for endogenous β-actin.

### 2.4. Immunofluorescence (IF)

One, 2, 5, 24 and 72 h after envenoming or saline administration the rats were killed with an overdose of anesthesia using a 3:1 mixture of ketamine chloride (Dopalen®, 100 mg/kg) and xylazine chloride (Anasedan®, 10 mg/kg). After that the rats were immediately perfused with 0.9% saline solution (100 ml) via the left ventricle followed by 4% paraformaldehyde in 0.1 M phosphate buffer, pH 7.4 (200 ml) as fixative. The cerebella were excised and immersed in 15% sucrose and then in 30% sucrose for cryoprotection (24 h each). Cerebellar samples were immersed in OCT-Tissue Tek (Sakura Finetek, Torrance, CA, USA) and frozen in *n*-hexane in liquid nitrogen (−70 °C). Frozen sections 5 μm thick were mounted on silanized glass slides and after rinsing with Trizma® buffer, pH 7.4, the slides were permeabilized with 0.1%

Triton X-100 for 10 min followed by incubation in phosphate-buffered 0.1% Tween 20 with 1% non-fat milk at room temperature to block non-specific antigens. The slides were incubated overnight with primary antibodies (anti-caveolin-1, 1:100; anti-dynamin-2, 1:50; anti-Src tyrosine kinase family, 1:100; anti-metalloproteinase-9, 1:50) diluted in blocking solution (phosphate-buffered 0.1% Tween 20 and 1% non-fat milk). After rinsing with phosphate buffer, the slides were incubated with the respective secondary antibodies conjugated with anti-rabbit Cy3 (Jackson ImmunoResearch Laboratories, Inc., West Grove, PA, USA) at room temperature (RT) for 45 min in the dark. The slides were then sealed using commercial sealant (Vectashield, Vetor Labs, Burlingame, CA, USA) and examined with fluorescent illumination in an Olympus BX51 photomicroscope (Olympus Corporation, Tokyo, Japan).

### 2.5. Transmission electron microscopy (TEM)

The thoracic cavity of anesthetized rats was opened and the left ventricle was exposed for perfusion with 0.9% saline solution (80 ml) to remove blood, followed by 250 ml of a fixative containing 2.5% paraformaldehyde and 2.5% glutaraldehyde in 0.1 M sodium cacodylate buffer, pH 7.2. After perfusion, the rats were stored at 4 °C for 12–18 h before removing the cerebellum in order to minimize changes to brain tissue. Subsequently, cerebellar fragments (0.5–1 mm) were immersed in the same fixative for 2 h at room temperature. The samples were then washed in a glucose solution (0.1 M sodium chloride plus 0.2 M sucrose) and post-fixed in 1% osmium tetroxide plus 1% potassium ferrocyanide in glucose solution for 1 h on ice. After rinsing with glucose solution, the samples were dehydrated in an increasing ethanol series until an ethanol/acetone ratio of 1:1 (v/v) was reached, followed by three baths (30 min each) in pure acetone. The samples were then embedded in acetone/resin (1:1) for 4 h and pure resin for 24 h under rotation. The final step involved polymerization in pure resin at 60 °C for 72 h. Semi-thin (0.5 μm thick) sections (Supernova LKB ultra-microtome, Bromma, Sweden) were stained with 0.5% toluidine blue for selection of the cerebellar regions by light microscopy. Ultrathin (60–70 nm) sections (Ultracut Reichert S, Leica, Wetzlar, Germany) collected on 200 mesh copper grids were contrasted with 2% uranyl acetate in methanol and 0.5% lead citrate in aqueous solution. Ultrastructural analyses were done with a transmission electron microscopy (Zeiss LEO 906, operated at 60 kV).

### 2.6. Statistical analysis

The results were expressed as the mean ± SEM and were analyzed using GraphPad Prism 5.0 (La Jolla, CA, USA). Differences between control and PNV-treated groups were assessed using Student's *t*-test with a value of $p \leq 0.05$ indicating significance. Two-way ANOVA followed by Bonferroni's post-hoc test was used to assess the impact of treatment and post-venom time interval on the observed alterations.

GraphPad Prism 5.0 software.

## 3. Results and discussion

In the present study, IF and WB was used to examine whether PNV upregulated or downregulated the expression of Cav-1, regardless of the stage of envenomation (initial or late) in which

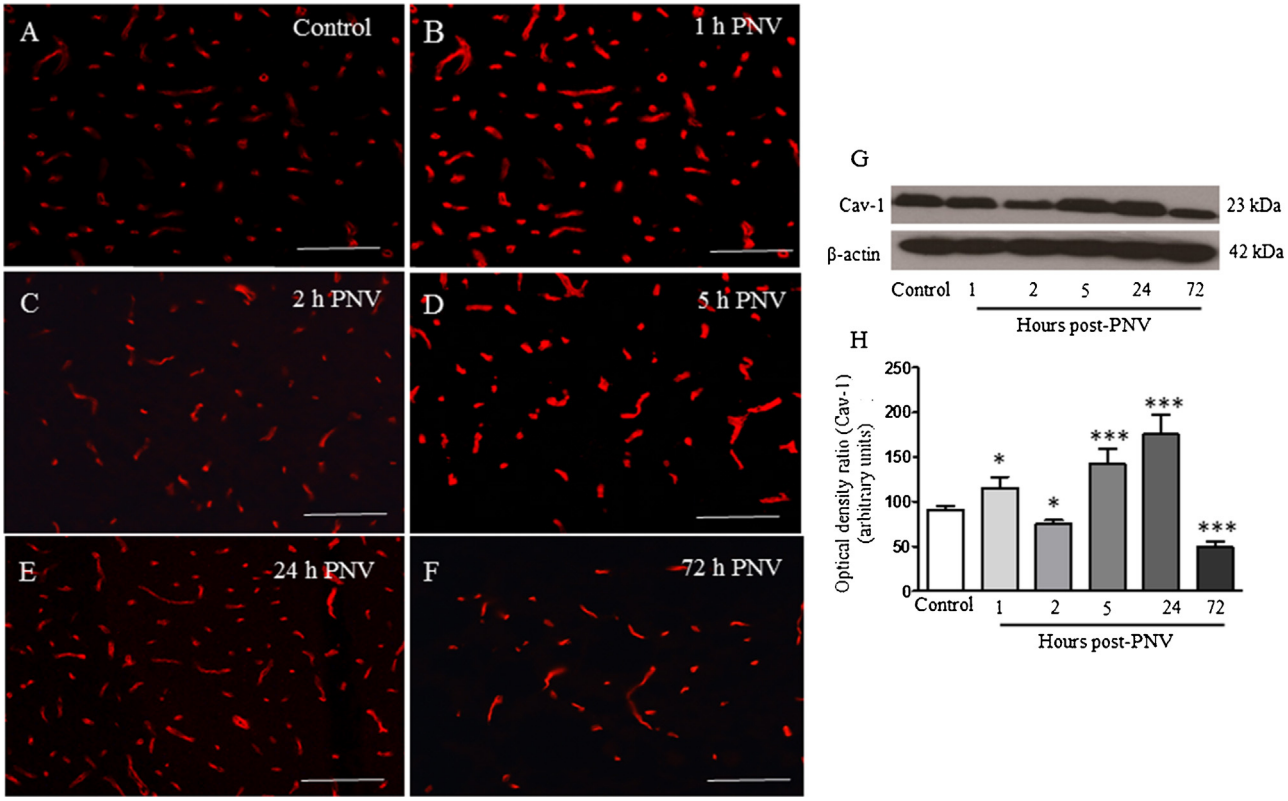


**Fig. 1.** Immunolabeling of caveolin-1 (Cav-1) in cerebellar tissue of rats injected i.v. with saline (A) or PNV (B–F). (G and H) Western blot of Cav-1 and histogram showing the density of the protein bands (normalized relative to β-actin). The columns are the mean ± SEM (n = 5), *$p \leq 0.05$, **$p \leq 0.01$ and *** $p \leq 0.001$ relative to control (Student's *t*-test). Bars: 40 μm.

the changes were elicited. In the cerebella of control rats, Cav-1 labeling was identified in 8–12-μm-wide capillaries; the venules and arterioles were Cav-1 negative (Fig. 1A). PNV induced time-dependent alterations in the expression of Cav-1, but only capillaries remained Cav-1 positive; maximum labeling occurred 1, 5 and 24 h after envenoming (Fig. 1B–F). WB data confirmed the changes in Cav-1 expression seen with IF. Significant increases were observed at 1, 5 and 24 h, while decreases were found at 2 h and 72 h (Fig. 1G–H). Two-way ANOVA revealed interactions between the variables time *vs.* treatment, indicating that the time elapsed after exposure to PNV influenced the venom-induced alterations ($p < 0.05$).

Caveolin 1, the main molecular marker of caveolae, is indispensable to the formation of caveolae and non-clathrin-coated endocytosis; deletion of Cav-1 impedes caveolar formation (Razani et al., 2002), the interaction of caveolae with other signal transduction proteins (see Quest et al., 2004) and accelerates neurodegeneration (Head et al., 2010). The downregulation and upregulation of Cav-1 expressed in the capillaries of PNV-treated rats implied an increased and decreased density of caveolae on the surface of endothelial cells and interference with plasma membrane dynamics. Indeed, TEM showed an increase in vesicle attachment to both the adluminal and abluminal membrane surface, in agreement with vesicle trafficking across the cerebellar endothelium of PNV-treated rats (Fig. 2). Ultrastructural findings corroborated the IF and WB data: an increase in Cav-1 expression implies that there was caveolar neoformation, whilst a reduction in Cav-1 implies caveolar flattening and internalization into the cytoplasm. Up- and downregulation of Cav-1 was also suggestive of cycles of membrane microdomain reassembly/disassembly during envenomation.

On the other hand, such caveolar dynamics imply tensional changes and mechanical stress in the endothelial membrane (Nassoy and Lamaze, 2012). Mechanical stress of the endothelial plasma membrane of brain capillaries is an important stimulus for triggering signaling mechanisms (Boyd et al., 2003) and presumably occurred in the present experiments.

Caveolae-derived vesicles and the internalization of caveolar content require the pCav-1 at an $NH_2$-terminal tyrosine residue by activation of the SKF (Shajahan et al., 2004b; Quest et al., 2004). This phosphorylation also requires interaction with Dyn2, a protein that forms the caveolar neck and participates in vesicle

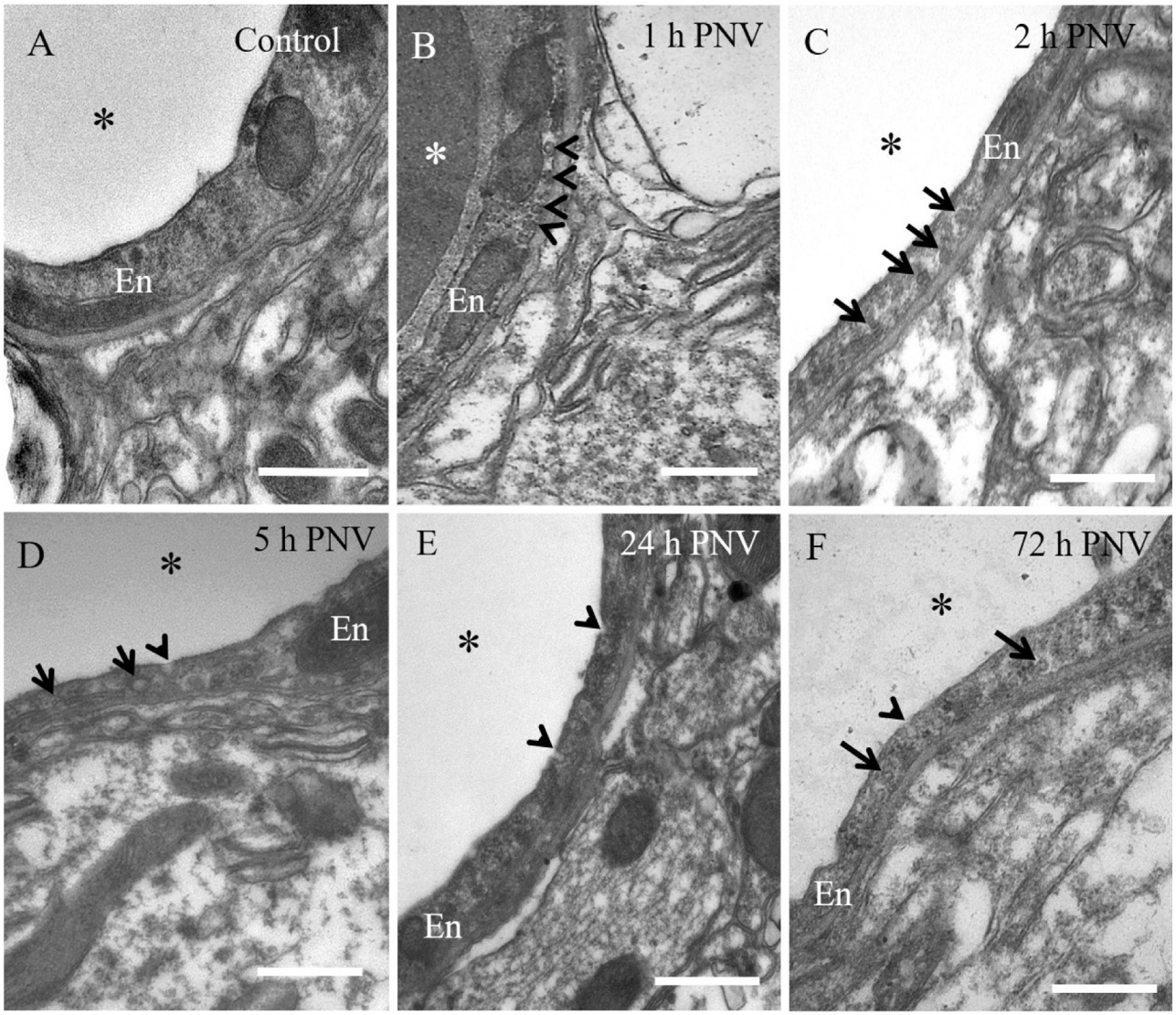


**Fig. 2.** Transmission electron microscopy images of the cerebellar endothelium of control rats (A) and at various intervals after injection of PNV (B–F). Asterisks = endothelial lumen; *arrowheads* show vesicles attached to adluminal and abluminal membrane surface; *arrows* indicate vesicles within the cytoplasm; A-like arrowheads (labeled in panels D–F) indicate newly caveolar-like endocytosis formation. En: endothelium. Bars: 500 nm.

detachment (membrane flattening) and internalization (Henley et al., 1998; Yao et al., 2005). In this context, we examined whether PNV induced phosphorylation of Cav-1 and altered SKF expression.

Immunolabeling of cytoplasmic SKF was detected in cells of the granular and molecular layers; relative to controls, PNV-injected rats showed upregulation of SKF, mainly at 2, 5 and 72 h; some venules were also SKF+ (Fig. 3A–F). WB for total SKF and pCav-1 in cerebellar homogenates revealed increases at 2 h and 72 h after envenoming and decreases at 1, 5 and 24 h after PNV (Fig. 3G–J). Two-way ANOVA revealed that expression of SKF and pCav-1 expression was affected by the variable time ($p \leq 0.05$).

The oscillating cycles of Cav-1 phosphorylation/dephosphorylation coupled to SKF upregulation/downregulation seen here in response to PNV suggested the triggering of a pathway of vesicular trafficking across the endothelium; the findings also suggested the occurrence of discontinuous vesicle shortage and internalization of the caveolar content over time. SKF activation also has a role in the participation of Dyn2 in the disassembly/reassembly of caveolae by inducing membrane flattening (detachment from plasma membrane) and neck reestablishment in the membrane caveolae (Shajahan et al., 2004a). Dyn2 interacts directly with Cav-1 and interferes with the internalization of caveolae (Yao et al., 2005).

Total Dyn2 protein expression increased at 5 h and 24 h after PNV and decreased at 2 h and 72 h (WB data). Dyn2 immunofluorescence appeared discontinuous in cerebellar vessels (Fig. 4A–H). Two-way ANOVA revealed that the time since PNV injection affected Dyn2 expression ($p \leq 0.05$). Curiously, the histogram profile that depicted the changes in Cav-1 over time mirrored that of Dyn2 exactly (compare Figs. 1 H with 4 H).

Dyn2 is ubiquitously expressed in a variety of vesicular structures, including synaptic, endocytic and phagocytic vesicles, as well as vesicles budding from Golgi lamellae and that form the neck of caveolae (González-Jamett et al., 2014). Such strategic locations have a direct role in membrane activity by serving as a point of release for vesicles (Henley et al., 1998). In the CNS, besides having a role in caveolar budding in the BBB (Oh et al., 1998), Dyn2 participates in synaptic vesicle recycling, post-synaptic receptor internalization, neurosecretion and preservation of synaptic transmission (reviewed by Yao et al., 2005; González-Jamett et al., 2014). Dyn2 is a large mechanochemical GTPase that interacts with multiple cellular proteins, including cytoskeletal proteins (Yao et al., 2005). We do not know whether alternating increases and decreases in proteins associated with caveolar dynamics in cerebellar capillary endothelium of PNV-treated rats created oscillatory frictional forces at the capillary wall, thereby triggering or inhibiting cell signal mechanisms. Despite, it could be an attractive possibility to explain some of the neurotoxic effects produced by *P. nigriventer* envenomation.

The matched upregulation/downregulation of Dyn2 and Cav-1 over time observed here suggests that the proteins that

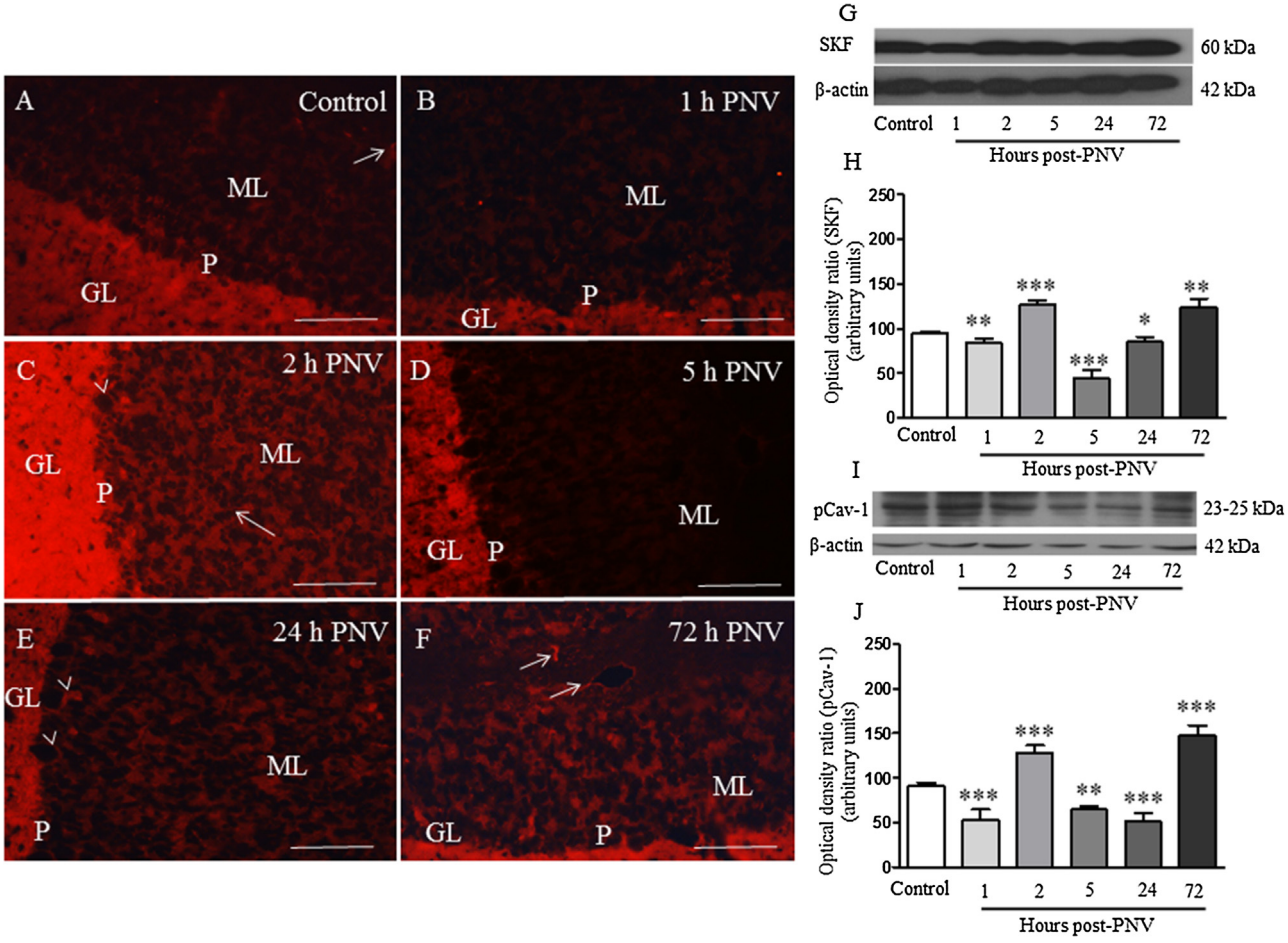


**Fig. 3.** Src tyrosine kinase family protein (SKF) expression in cerebellar tissue of rats injected i.v. with saline (control) (A) or PNV (B–F). (G and I) Western blots of SKF and phosphorylated caveolin-1 (pCav-1) and (H and J) respective histograms showing the density of the protein bands (normalized relative to β-actin). The columns are the mean ± SEM (n = 5), *$p \leq 0.05$, **$p \leq 0.001$ and ***$p \leq 0.001$ relative to the control (Student's *t*-test). ML, molecular layer; GL, granular layer; P, Purkinje layer; *Arrows* indicate labeled endothelium. *Arrows head* indicate Purkinje cells labeling. Bars: 40 μm.

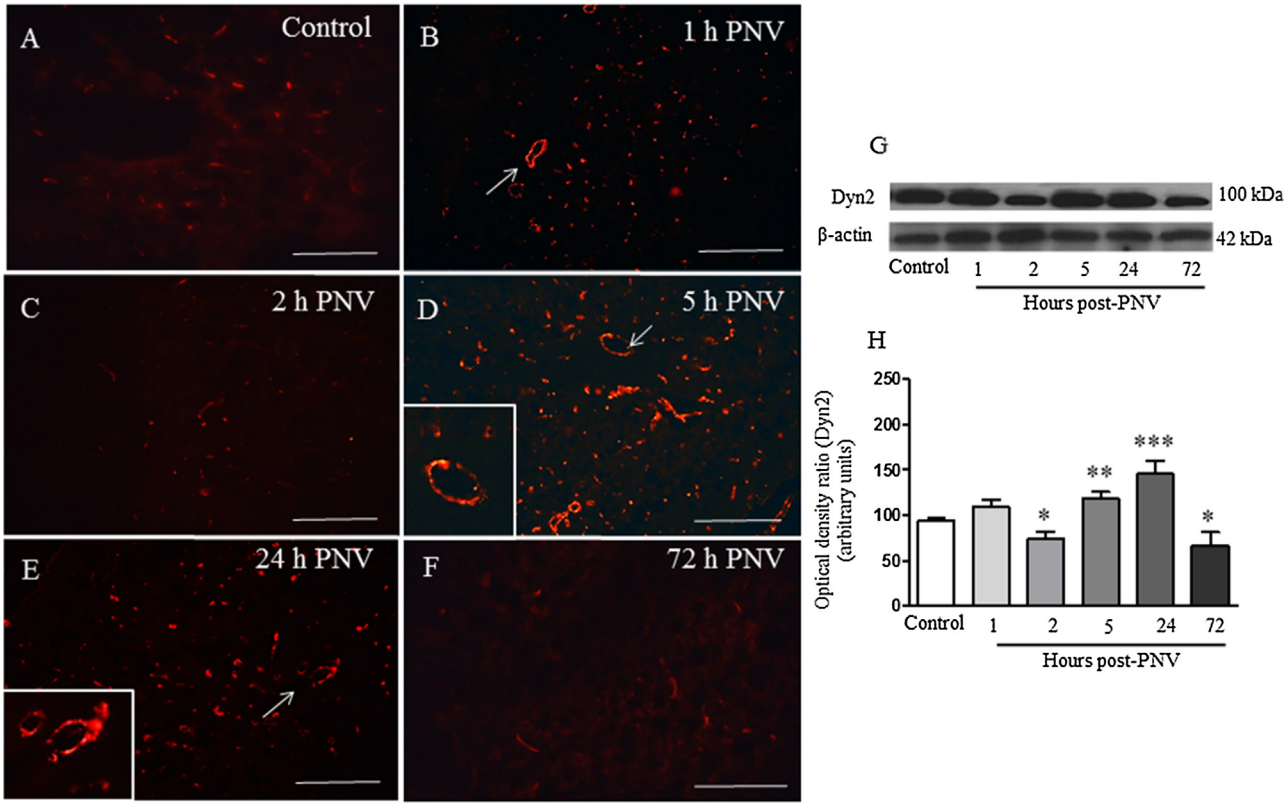


**Fig. 4.** Dyn2 protein expression in cerebellar tissue of rats injected i.v. with saline (control) (A) or PNV (B–F). (G and H) Western blot of Dyn2 and respective histogram showing the density of the protein bands (normalized relative to β-actin); *arrows* indicate endothelium labeling. The columns are the mean ± SEM (n = 5), $^{*}p \leq 0.05$, $^{**}p \leq 0.001$ and $^{***}p \leq 0.001$ relative to the control (Student's *t*-test). Bars: 40 μm.

form the caveolar neck and vesicle body are synchronized in response to PNV. Intriguingly, Dyn2 (and thus Cav-1) upregulation/downregulation was asynchronous relative to the SKF and pCav-1 counterparts (compare the histograms in Fig. 3H, J with that of Fig. 4H). Based on this observation, we suggest that caveolar disassembly (SKF/pCav-1 activation) and reassembly (increased expression of Cav-1 and Dyn2) altered local vascular hemodynamics and caused mechano-transduction of signals that affected BBB permeability. Indeed, a number of studies have established a connection between caveolae as endothelial mechanosensors of shear stress and their luminal membrane location (Boyd et al., 2003; Rizzo et al., 2003; Nassoy and Lamaze, 2012; Parton and del Pozo, 2013) and BBB permeability. Shear stress also affects the activation of ERK and AKT, two well-known shear-detecting signaling molecules (Boyd et al., 2003).

Shear stress resulting from changes in hemodynamic parameters also affects endothelial nitric oxide synthase (eNOS), a signaling molecule compartmentalized in the caveolar microdomain (Rizzo et al., 1998; Rath et al., 2009). In the same experimental model as used here, we have previously shown that eNOS is inactivated during periods of critical periods of envenoming (1 h and 2 h) by PNV through the venom's ability to disrupt the active dimeric form. At 24 and 72 h, periods of no clinical manifestation of intoxication of rats, eNOS recoupling achieved higher levels (Soares et al., 2015). eNOS is negatively regulated by Cav-1 (García-Cardeña et al., 1997), but inhibition of this enzyme is blocked by a rise in intracellular calcium levels. Increased intracellular calcium as induced by some PNV toxins (Romano-Silva et al., 1993), promotes the binding of calmodulin to eNOS enzyme resulting in catalytic activity (Förstermann and Sessa, 2012) and NO bioavailability. Based on these observations, we suggest that during periods of severe envenomation, the lower availability of nitric oxide on the one hand and the positive regulation of endocytosis and transcytosis on the other hand contributes to enhanced BBB permeability and vascular dysfunction in response to PNV.

We have previously shown that in addition to BBB breakdown, PNV decreases the laminin content of the endothelial basement membrane (Rapôso et al., 2007; Mendonça et al., 2013) and increases the expression of tumor necrosis factor alpha (TNFα) and interferon gamma (IFNγ) in rat cerebellum and hippocampus (da Cruz-Höfling et al., 2009). During brain injury, the activation of matrix metalloproteinases (MMPs) degrades the extracellular matrix surrounding blood microvessels (basement membrane) and permeabilizes the BBB (Gu et al., 2011). A recent study established a link between MMP9 activity and caveolar transcytosis and BBB permeation (Muradashvili et al., 2014). The authors reported a direct relationship between caveolar formation, assessed by increased Cav-1 expression, and the activation of MMP9; the inhibition of MMP9 activity preserved the intactness of the BBB.

In this study, we examined the effect of PNV on MMP9 expression in an attempt to relate this to the expression of Cav-1, pCav-1, Dyn2 and SKF in the cerebellum of PNV-treated rats. MMP9 expression increased 1, 5 and 24 h after PNV injection, was unaltered at 2 h and decreased at 72 h (Fig. 5G and H). Treatment with PNV increased the immunodetection of MMP9, which peaked at 24 h and declined substantially at 72 h (Fig. 5A–F). Two-way ANOVA revealed interactions between the variables times *vs.* treatment in MMP9 expression, indicating that the time

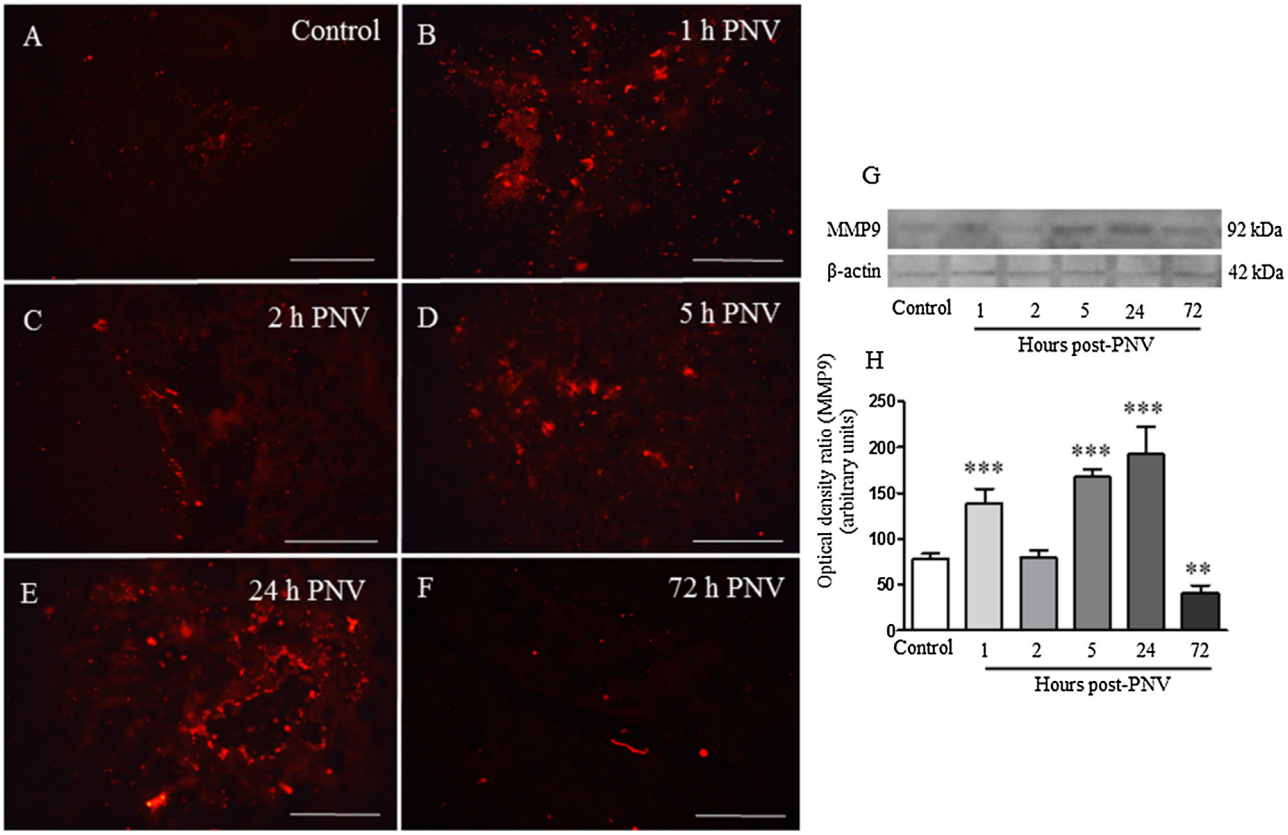


**Fig. 5.** MMP9 protein expression in cerebellar tissue of rats injected with saline (control) (A) or PNV (B–F). (G and H) Western blot of MMP9 and respective histogram showing the density of the protein bands (normalized relative to β-actin). The columns are the mean ± SEM (n = 5), *$p \leq 0.05$, **$p \leq 0.001$ and ***$p \leq 0.001$ relative to the control (Student's *t*-test). Bars: 40 μm.

elapsed after PNV injection influenced the effect of the venom ($p \leq 0.05$).

Overall, our findings indicate that Cav-1, Dyn2 and MMP9 expression was synchronously upregulated and down-regulated in response to PNV, and that these changes were asynchronous to those of SKF and pCav-1 expression. There was a direct relationship between the peaks of MMP9 expression and those of caveolae formation, as assessed based on the peaks of Cav-1 and Dyn2 expression. The peaks of Cav-1, Dyn2 and MMP9 expression coincided with minor expressions of pCav-1 and SKF.

In summary, the results described in this report provide evidence that in rats PNV can induce a pro-inflammatory state and trigger signaling via caveolae to enhance transport across the BBB. We suggest that PNV-induced cycling between caveolar disassembly (SKF/pCav-1 activation) and reassembly (increased expression of Cav-1 and Dyn2) adversely affects the hemodynamics of the BBB, thereby altering the permeability of this structure. Given the role of caveolar dynamics in shear stress and the regulation of BBB permeability, the modulation of caveolar formation and cycling could be a relevant therapeutic target for treating human envenomation by *P. nigriventer*.

## Conflict of interest

The authors declared no conflict of interest.

## Acknowledgments

The authors thank Miguel Silva and Antonio Vilson dos Santos for excellent animal care and Stephanie Souto Mayor for technical assistance. The work was supported by grants from Brazilian foundations, Fundação de Amparo à Pesquisa do Estado de São Paulo (FAPESP, grant no. 2005/53625-1) and Conselho Nacional de Desenvolvimento Científico e Tecnológico (CNPq grant no. 486142/2012-4). E.S.S. was supported by a studentship from CNPq and M.C.P.M. by a studentship from FAPESP (grant no. 2012/24782-5). M.A.C.H. is supported by a CNPq research fellowship (grant no. 305099/2011-6). This is study is part of an MSc dissertation by E.S. S. None of the funding agencies indicated above was involved in the study design, in data collection, analysis and interpretation, in writing the report and in the decision to submit the article for publication. We are indebted to Professor Stephen Hyslop who provided editorial assistance with the English of the manuscript.

## References

Boyd, N.L., Park, H., Yi, H., Boo, Y.C., Sorescu, G.P., Sykes, M., Jo, H., 2003. Chronic shear induces caveolae formation and alters ERK and Akt responses in endothelial cells. Am. J. Physiol. Heart Circ. Physiol. 285, H1113–H1122.

Bucaretchi, F., Reinaldo, C.R.D., Hyslop, S., Madureira, P.R., de Capitani, E.M., Vieira, R. J., 2000. A clinic-epidemiological study of bites by spiders of the genus *Phoneutria*. Rev. Inst. Med. Trop. São Paulo 42, 17–21.

Bucaretchi, F., Mello, S.M., Vieira, R.J., Mamoni, R.L., Blotta, M.H., Antunes, E., Hyslop, S., 2008. Systemic envenomation caused by the wandering spider *Phoneutria nigriventer*, with quantification of circulating venom. Clin. Toxicol. 46, 885–889.

da Cruz-Höfling, M.A., Rapôso, C., Verinaud, L., Zago, G.M., 2009. Neuroinflammation and astrocytic reaction in the course of *Phoneutria nigriventer* (armed-spider) blood-brain barrier (BBB) opening. Neurotoxicology 30, 636–646.

Förstermann, U., Sessa, W.C., 2012. Nitric oxide synthases: regulation and function. Eur. Heart J. 33, 829–837. doi:http://dx.doi.org/10.1093/eurheartj/ehr304.

Fontana, M.D., Vital-Brazil, O., 1985. Mode of action of *Phoneutria nigriventer* spider venom at the isolated phrenic nerve-diaphragm of the rat. Braz. J. Med. Biol. Res. 18, 557–565.

García-Cardeña, G., Martasek, P., Masters, B.S., Skidd, P.M., Couet, J., Li, S., Lisanti, M. P., Sessa, W.C., 1997. Dissecting the interaction between nitric oxide synthase (NOS) and caveolin: functional significance of the NOS caveolin binding domain *in vivo*. J. Biol. Chem. 272, 25437–25440.

Gomez, M.V., Kalapothakis, E., Guatimosim, C., Prado, M.A., 2002. *Phoneutria nigriventer* venom: a cocktail of toxins that affect ion channels. Cell. Mol. Neurobiol. 22, 579–588.

González-Jamett, A.M., Haro-Acuña, V., Momboisse, F., Caviedes, P., Bevilacqua, J.A., Cárdenas, A.M., 2014. Dynamin-2 in nervous system disorders. J. Neurochem. 128, 210–223.

Gu, Y., Dee, C.M., Shen, J., 2011. Interaction of free radicals, matrix metalloproteinases and caveolin-1 impacts blood-brain barrier permeability. Front. Biosci. (School Ed.). 3, 1216–1231.

Head, B.P., Peart, J.N., Panneerselvam, M., Yokoyama, T., Pearn, M.L., Niesman, I.R., Bonds, J.A., Schilling, J.M., Miyanohara, A., Headrick, J., Ali, S.S., Roth, D.M., Patel, P.M., Patel, H.H., 2010. Loss of caveolin-1 accelerates neurodegeneration and aging. PLoS One 5, e15697.

Henley, J.R., Krueger, E.W.A., Oswald, B.J., McNiven, M.A., 1998. Dynamin-mediated internalization of caveolae. J. Cell Biol. 141, 85–99.

Le Sueur, L.P., Kalapothakis, E., Cruz-Höfling, M.A., 2003. Breakdown of the blood-brain barrier and neuropathological changes induced by *Phoneutria nigriventer* spider venom. Acta Neuropathol. 2, 125–134.

Le Sueur, L.P., Collares-Buzato, C.B., Cruz-Höfling, M.A., 2004. Mechanisms involved in the blood-brain barrier increased permeability induced by *Phoneutria nigriventer* spider venom in rats. Brain Res. 1027, 38–47.

Le Sueur, L., Collares-Buzato, C.B., Kalapothakis, E., Cruz-Höfling, M.A., 2005. In vitro effect of the *Phoneutria nigriventer* spider venom on cell viability paracellular barrier function and transcellular transport in cultured cell lines. Toxicon 46, 130–141.

Love, S., Cruz-Höfling, M.A., Duchen, L.W., 1986. Morphological abnormalities in myelinated nerve fibres caused by *Leiurus*, *Centruroides* and *Phoneutria* venoms and their prevention by tetrodotoxin. Q. J. Exp. Physiol. 71, 115–122.

Mendonça, M.C., Soares, E.S., Stávale, L.M., Irazusta, S.P., da Cruz-Höfling, M.A., 2012. Upregulation of the vascular endothelial growth factor, Flt-1, in rat hippocampal neurons after envenoming by *Phoneutria nigriventer*: age-related modulation. Toxicon 60, 656–664.

Mendonça, M.C., Soares, E.S., Stávale, L.M., Rapôso, C., Coope, A., Kalapothakis, E., da Cruz-Höfling, M.A., 2013. Expression of VEGF and Flk-1 and Flt-1 receptors during blood-brain barrier (BBB) impairment following Phoneutria nigriventer spider venom exposure. Toxins 5, 2572–2588.

Mendonça, M.C., Soares, E.S., Stávale, L.M., Kalapothakis, E., da Cruz-Höfling, M.A., 2014. Vascular endothelial growth factor increases during blood-brain barrier-enhanced permeability caused by *Phoneutria nigriventer* spider venom. Biomed. Res. Int. 2014, 721968. doi:http://dx.doi.org/10.1155/2014/721968.

Muradashvili, N., Benton, R.L., Tyagi, R., Tyagi, S.C., Lominadze, D., 2014. Elevated level of fibrinogen increases caveolae formation: role of matrix metalloproteinase-9. Cell Biochem. Biophys. 69 (2), 283–294.

Nag, S., Manias, J.L., Stewart, D.J., 2009. Expression of endothelial phosphorylated caveolin-1 is increased in brain injury. Neuropathol. Appl. Neurobiol. 35, 417–426.

Nassoy, P., Lamaze, C., 2012. Stressing caveolae new role in cell mechanics. Trends Cell Biol. 22, 381–389.

Oh, P., McIntosh, D., Schnitzer, J.E., 1998. Dynamin at the neck of caveolae mediates their budding to form transport vesicles by GTP-driven fission from the plasma membrane of endothelium. J. Cell Biol. 141, 101–114.

Parton, R.G., del Pozo, M.A., 2013. Caveolae as plasma membrane sensors, protectors and organizers. Nat. Rev. Mol. Cell Biol. 14, 98–112.

Pattel, H.H., Murray, F., Insel, P.A., 2008. Caveolae as organizers of pharmacologically relevant signal transduction molecules. Annu. Rev. Pharmacol. Toxicol. 48, 359–391.

Pelkmans, L., Helenius, A., 2002. Endocytosis via caveolae. Traffic 3, 311–320.

Quest, A.F.G., Leyton, L., Párraga, M., 2004. Caveolins, caveolae, and lipid rafts in cellular transport, signaling and disease. Biochem. Cell Biol. 82, 129–144.

Rapôso, C., Odorissi, P.A., Oliveira, A.L., Aoyama, H., Ferreira, C.V., Verinaud, L., Fontana, K., Ruela-de-Sousa, R.R., da Cruz-Höfling, M.A., 2012. Effect of Phoneutria nigriventer venom on the expression of junctional protein and P-gp efflux pump function in the blood-brain barrier. Neurochem. Res. 37, 1967–1981.

Rapôso, C., Odorissi, P.A., Savioli, S.F., Hell, R.C., Simões, G.F., Ruela-de-Sousa, R.R., de Oliveira, A.L., da Cruz-Höfling, M.A., 2014. Triggering of protection mechanism against Phoneutria nigriventer spider venom in the brain. PLoS One 9, e107292.

Rapôso, C., Zago, G.M., da Silva, G.H., Cruz-Höfling, M.A., 2007. Acute blood-brain barrier permeabilization in rats after systemic Phoneutria nigriventer venom. Brain Res. 1149, 18–29.

Rath, G., Dessy, C., Feron, O., 2009. Caveolae, caveolin and control of vascular tone: nitric oxide (NO) and endothelium derived hyperpolarizing factor (EDHF) regulation. J. Physiol. Pharmacol. 60 (Suppl. 4), 105–109.

Razani, B., Combs, T.P., Wang, X.B., Frank, P.G., Park, D.S., Russel, R.G., Li, M., Tang, B., Jelicks, L.A., Scherer, P.E., Lisanti, M.P., 2002. Caveolin-1-deficient mice are lean, resistant to diet-induced obesity, and show hypertriglyceridemia with adipocyte abnormalities. J. Biol. Chem. 277, 8635–8647.

Rizzo, V., McIntosh, D.P., Oh, P., Schnitzer, J.E., 1998. In situ flow activates endothelial nitric oxide synthase in luminal caveolae of endothelium with rapid caveolin dissociation and calmodulin association. J. Biol. Chem. 273, 34724–34729.

Rizzo, V., Morton, C., DePaola, N., Schnitzer, J.E., Davies, P.F., 2003. Recruitment of endothelial caveolae into mechanotransduction pathways by flow conditioning *in vitro*. Am. J. Physiol. Heart Circ. Physiol. 285, H1720–9.

Romano-Silva, M.A., Ribeiro-Santos, R., Ribeiro, A.M., Gomez, M.V., Diniz, C.R., Cordeiro, M.N., Brammer, M.J., 1993. Rat cortical synaptosomes have more than one mechanism for Ca2+ entry linked to rapid glutamate release: studies using the *Phoneutria nigriventer* toxin PhTX2 and potassium depolarization. Biochem. J 296, 313–319.

Shajahan, A.N., Timblin, B.K., Sandoval, R., Tiruppathi, C., Malik, A.B., Minshall, R.D., 2004a. Role of Src-induced dynamin-2 phosphorylation in caveolae-mediated endocytosis in endothelial cells. J. Biol. Chem. 279, 20392–20400.

Shajahan, A.N., Tiruppathi, C., Smrcka, A.V., Malik, A.B., Minshall, R.D., 2004b. Gβγ activation of Src induces caveolae-mediated endocytosis in endothelial cells. J. Biol. Chem. 279, 48055–48062.

Soares, E.S., Mendonça, M.C., Stávale, L.M., Irasusta, S.P., Coope, A., Cruz-Höfling, M. A., 2014. Evidences of endocytosis via caveolae following blood–brain barrier breakdown by *Phoneutria nigriventer* spider venom. Toxicol. Lett. 229, 415–422.

Soares, E.S., Mendonça, M.C., Cruz-Höfling, M.A., 2015. eNOS uncoupling in the cerebellum after BBB disruption by exposure to *Phoneutria nigriventer* spider venom. Toxicon 104, 7–13. doi:http://dx.doi.org/10.1016/j.toxicon.2015.07.009.

Stávale, L.M., Soares, E.S., Mendonça, M.C., Irazusta, S.P., da Cruz Höfling, M.A., 2013. Temporal relationship between aquaporin-4 and glial fibrillary acidic protein in cerebellum of neonate and adult rats administered a BBB disrupting spider venom. Toxicon 66, 37–46.

Stern, C.M., Mermelstein, P.G., 2010. Caveolin regulation of neuronal intracellular signaling. Cell. Mol. Life Sci. 67, 3785–3795.

Yao, Q., Chen, J., Cao, H., Orth, J.D., McCaffery, J.M., Stan, R.V., McNiven, M.A., 2005. Caveolin-1 interacts directly with dynamic-2. J. Mol. Biol. 348, 491–501.